

## Tight-binding study of the anomalous phonon spectrum of barium

K. Schwartzman

*Department of Physics, Indiana University of Pennsylvania, Indiana, Pennsylvania 15705*

P. C. Pattnaik

*IBM Thomas J. Watson Research Center, Yorktown Heights, New York 10598*

(Received 11 February 1988)

The long-range contribution to the phonon dynamical matrix for bcc Ba is calculated from first principles using a perturbative tight-binding formulation of the electron-ion interaction. This contribution gives rise to excellent agreement with the anomalous neutron-scattering spectrum in which the longitudinal mode is found to lie at lower frequencies than the transverse mode in the [100] direction. The short-range contribution is treated within a force-constant model and is not responsible for anomalous behavior in the spectrum. In addition,  $p$ - $d$  and  $d$ - $d$  mixing terms in the electron-phonon matrix elements form the majority contribution to the dynamical matrix, suggesting that Ba behaves as a transition metal with regard to its electron-phonon interaction. This is similar to previous results obtained from nonperturbative calculations of the total crystal energy.

### I. INTRODUCTION

Considerable interest has recently developed in the anomalous phonon spectrum of bcc Ba.<sup>1-4</sup> As observed in neutron-scattering measurements,<sup>1</sup> the longitudinal mode of the spectrum lies lower in frequency than the transverse mode in the [100] direction. Within the limits of experimental accuracy, this behavior begins at approximately  $0.2\pi/a$  and persists to the degeneracy at the  $H$  point on the zone boundary. It is all the more interesting since neither Ca nor Sr exhibits such unusual behavior. Several early empirical calculations<sup>5-7</sup> of the spectrum did not indicate the presence of this anomaly. Two subsequent studies,<sup>2,3</sup> however, in which first-principles calculations of the total crystal energy were made, could account for the observed features by inclusion of  $5d$  electron effects. The two differed insofar as the first<sup>2</sup> found hybridization of the unoccupied  $5d$  band with the conduction band responsible for the anomalous behavior, while the second<sup>3</sup> attributed this behavior to partial occupation of the  $5d$  band. More recently it has been suggested<sup>4</sup> that the unusual spectrum arises from exchange coupling between the conduction band and the  $5s$  and  $5p$  states. It is the purpose of the present study to reexamine this question in order to understand the source of the anomaly.

The approach taken here specifically focuses on the long-range contribution to the phonon dynamical matrix by calculating it from first principles. Since this contribution is generally responsible for anomalous phonon structure, its evaluation can help shed light on the physical origin of such structure in Ba. It may be isolated from the full dynamical matrix by judiciously separating<sup>8,9</sup> the total crystal energy into its long- and short-range contributions. This was first exploited by Varma, Weber, and co-workers<sup>8,9</sup> in studies of the electron-phonon interaction in transition metals. Taking gra-

dients of the crystal energy in order to obtain the dynamical matrix, one finds

$$D_{\alpha\beta}(\mathbf{q}) = D_{\alpha\beta}^{(0,1)}(\mathbf{q}) + D_{\alpha\beta}^{(2)}(\mathbf{q}), \quad (1)$$

where  $D^{(0,1)}$  and  $D^{(2)}$  are the short- and long-range contributions, respectively. The short-range part is not important as a source of anomalous behavior and may be accurately treated within a force-constant model.<sup>10</sup> As discussed below, the parameters of the model are determined using the measured elastic constants and the observed phonon frequency at the  $H$  point.

The  $D^{(2)}$  contribution to the phonon dynamical matrix can be written as the static real part of a fully dressed phonon self-energy insertion with screened Coulomb vertices at *both* ends. Since Coulomb vertex *dynamics* may be reasonably neglected for the real parts of these self-energies, the electron-phonon coupling itself can be taken, in principle, as both fully renormalized and static.<sup>11</sup> With virtually no loss of generality,  $D^{(2)}$  may then be treated within the random-phase approximation (RPA). Thus,

$$D_{\alpha\beta}^{(2)}(\mathbf{q}) = - \sum_{\mathbf{k}, \mu, \mu'} \frac{f_{\mathbf{k}\mu} - f_{\mathbf{k}+\mathbf{q}\mu'}}{E_{\mathbf{k}\mu} - E_{\mathbf{k}+\mathbf{q}\mu'}} \times g_{\mathbf{k}\mu, \mathbf{k}+\mathbf{q}\mu'}^{\alpha} g_{\mathbf{k}+\mathbf{q}\mu', \mathbf{k}\mu}^{\beta}, \quad (2)$$

where  $E_{\mathbf{k}\mu}$  is the band energy for wave vector  $\mathbf{k}$  and band index  $\mu$ , and  $f_{\mathbf{k}\mu}$  is the equilibrium Fermi occupation factor for this energy. The electron-phonon coupling between the electronic states  $(\mathbf{k}, \mu)$  and  $(\mathbf{k} + \mathbf{q}, \mu')$  for ionic motion in the Cartesian direction  $\alpha$  ( $\alpha = x, y, z$ ) is, in the orthogonal tight-binding approximation,<sup>12</sup>

$$g_{\mathbf{k}\mu, \mathbf{k}+\mathbf{q}\mu'}^{\alpha} = \sum_{m,n} A_{m\mu}^{\dagger}(\mathbf{k}) [\gamma_{mn}^{\alpha}(\mathbf{k}) - \gamma_{mn}^{\alpha}(\mathbf{k} + \mathbf{q})] \times A_{n\mu'}(\mathbf{k} + \mathbf{q}), \quad (3)$$

where the “ $\gamma$  matrices” are written

$$\gamma_{mn}^{\alpha}(\mathbf{k}) = \sum_{\mathbf{R}_{ij}} e^{i\mathbf{k}\cdot\mathbf{R}_{ij}} \nabla_{\alpha} H_{im,jn} \quad (4)$$

and  $H_{im,jn}$  is the tight-binding Hamiltonian matrix element between the atomic orbitals  $|m\rangle$  at the lattice site  $i$  and  $|n\rangle$  at the site  $j$ . The eigenvectors  $\mathbf{A}_{\mu}(\mathbf{k})$  in Eq. (3), as well as the band energies, are determined in principle from a self-consistent solution to the electronic Schrödinger equation. It should be pointed out now, however, that the successful application of the tight-binding method requires relatively localized atomic  $d$  states. Conversely, an accurate calculation of the phonon spectrum of Ba using this approach is suggestive of the transition metal character of the electron-phonon interaction in this metal.

Straightforward evaluation of the Brillouin zone sum in Eq. (2) is very time consuming and it is necessary to employ techniques which minimize this time. It is convenient to begin by restricting the sum to the irreducible ( $\frac{1}{48}$ ) portion of the Brillouin zone (IBZ). Equation (2) can then be written in the form

$$D_{\alpha\beta}^{(2)}(\mathbf{q}) = - \sum_{\hat{\eta}, \mathbf{k} \in \text{IBZ}, \mu, \mu'} \frac{f_{\hat{\eta}\mathbf{k}\mu} - f_{\hat{\eta}\mathbf{k}+\mathbf{q}\mu'}}{E_{\hat{\eta}\mathbf{k}\mu} - E_{\hat{\eta}\mathbf{k}+\mathbf{q}\mu'}} g_{\hat{\eta}\mathbf{k}\mu, \hat{\eta}\mathbf{k}+\mathbf{q}\mu'}^{\alpha} \times g_{\hat{\eta}\mathbf{k}+\mathbf{q}\mu', \hat{\eta}\mathbf{k}\mu}^{\beta}, \quad (5)$$

where the  $\mathbf{k}$  are taken to lie in the IBZ and the  $\hat{\eta}$  sum runs through the 48 transformations that map the IBZ into the full first zone. The Fermi factors are functions

only of the band energies and these are invariant under transformation into an equivalent point in the zone:

$$E_{\hat{\eta}\mathbf{k}\mu} = E_{\mathbf{k}\mu}. \quad (6a)$$

Similarly,

$$E_{\hat{\eta}\mathbf{k}+\mathbf{q}\mu'} = E_{\mathbf{k}+\mathbf{q}\mu'}, \quad (6b)$$

where  $\mathbf{q}' \equiv \hat{\eta}^{-1}\mathbf{q}$ . The eigenvectors and  $\gamma$  matrices transform according to

$$\mathbf{A}(\hat{\eta}\mathbf{k}) = \hat{\eta} \mathbf{A}(\mathbf{k}) \quad (7a)$$

and

$$\gamma_{mn}^{\alpha}(\hat{\eta}\mathbf{k}) = \sum_{\alpha', m', n'} \eta_{\alpha\alpha'} \eta_{mm'} \eta_{nn'} \gamma_{m'n'}^{\alpha'}(\mathbf{k}), \quad (7b)$$

respectively. In Eqs. (7a) and (7b), the transformations  $\eta_{mm'}$  and  $\eta_{nn'}$  are in the orbital representation for any element of the point symmetry group of  $\mathbf{k}$ ; only the spatial part of  $\hat{\eta}$  is necessary to understand the transformation properties of the other quantities used here. In terms of Eqs. (7a) and (7b), the electron-phonon coupling can be seen to transform as

$$g_{\hat{\eta}\mathbf{k}\mu, \hat{\eta}\mathbf{k}+\mathbf{q}\mu'}^{\alpha} = \sum_{\alpha'} \eta_{\alpha\alpha'} g_{\mathbf{k}\mu, \mathbf{k}+\mathbf{q}\mu'}^{\alpha'} \quad (8)$$

and so the transformation characteristics of the summand in Eq. (5) are established.

Using Eqs. (6)–(8), the  $D^{(2)}$  contribution to the dynamical matrix becomes

$$D_{\alpha\beta}^{(2)}(\mathbf{q}) = - \sum_{\hat{\eta}, \alpha', \beta'} \eta_{\alpha\alpha'} \eta_{\beta\beta'} \sum_{\mathbf{k} \in \text{IBZ}, \mu, \mu'} \frac{f_{\mathbf{k}\mu} - f_{\mathbf{k}+\mathbf{q}\mu'}}{E_{\mathbf{k}\mu} - E_{\mathbf{k}+\mathbf{q}\mu'}} g_{\mathbf{k}\mu, \mathbf{k}+\mathbf{q}\mu'}^{\alpha'} g_{\mathbf{k}+\mathbf{q}\mu', \mathbf{k}\mu}^{\beta'} \quad (9)$$

While the effort required to perform the wave-vector sum has been reduced considerably, it may appear that this has been accomplished only at the expense of having to sum over the  $\hat{\eta}$ . However, it is generally of interest to consider the  $\mathbf{q}$  lying only along symmetry directions. In this case, there are significantly fewer than 48 distinct wave vectors  $\mathbf{q}'$ . For  $\mathbf{q}$  in the [100] direction there are only six distinct  $\mathbf{q}'$ , and so the band structure and electron-phonon couplings appearing in Eq. (9) have only to be evaluated for six different combinations of  $\mathbf{k} + \mathbf{q}'$  for each  $\mathbf{k}$  in the IBZ. (For  $\mathbf{q}$  in the [111] or [110] directions, there are 8 and 12 discrete  $\mathbf{q}'$ , respectively.) It should be noted that even this is not necessary if  $\mathbf{q}$  is coincident with one of the  $\mathbf{k}$ , for then the band structure and electron-phonon coupling need to be evaluated only once. Equation (9) can then be computed using the transformation properties of the integrand for the 48  $\hat{\eta}$ . However, it is often necessary to probe finer details of the spectrum in studying anomalous phonon structure. As a result, advantage is not taken of this last simplification in the present study.

The  $D^{(2)}$  calculation is performed by evaluating Eq. (9). The band energies and eigenvectors are determined from a 34-parameter orthogonal two-center Slater-Koster fit to a first-principles scalar relativistic APW band structure

for Ba.<sup>13</sup> The fit is accurate to 0.07 eV overall and is accomplished using a nine-element (one  $s$ , three  $p$ , and five  $d$ ) basis set. The Slater-Koster band structure is shown in Fig. 1 for high symmetry directions and it bears a strong similarity to the first-principles pseudopotential band structure found in Ref. 2. This band structure also yields the result, as in Ref. 2, that the  $d$  states contribute significantly to the electronic density of states.

In order to compute the  $\gamma$  matrices, the gradient in Eq. (4) is separated into its radial and angular parts. The radial parts are conveniently treated using the Harrison scaling scheme<sup>14</sup> in which the bond parameters are taken to vary as powers of the bond length  $r$ : the  $s$ - $s$ ,  $s$ - $p$ , and  $p$ - $p$  bonds vary as  $r^{-2}$ , the  $s$ - $d$  and  $p$ - $d$  bonds as  $r^{-7/2}$ , and the  $d$ - $d$  bonds as  $r^{-5}$ . Using this scaling both the radial and angular parts of the gradient can be evaluated analytically. The  $\gamma$  matrices are then found by taking the lattice sum in Eq. (4) up to third nearest neighbor and the electron-phonon coupling is calculated directly. Finally, the wave-vector sum in Eq. (9) is carried out at zero temperature (where the Fermi factors may be treated as  $\theta$  functions) using the analytical tetrahedron method<sup>15</sup> for 506  $\mathbf{k}$  points in the IBZ. Accuracy is ensured by allowing the band energies and matrix elements (i.e.,  $g^{\alpha\beta}$ ) to vary linearly within the tetrahedra (2000 in the IBZ). Tests

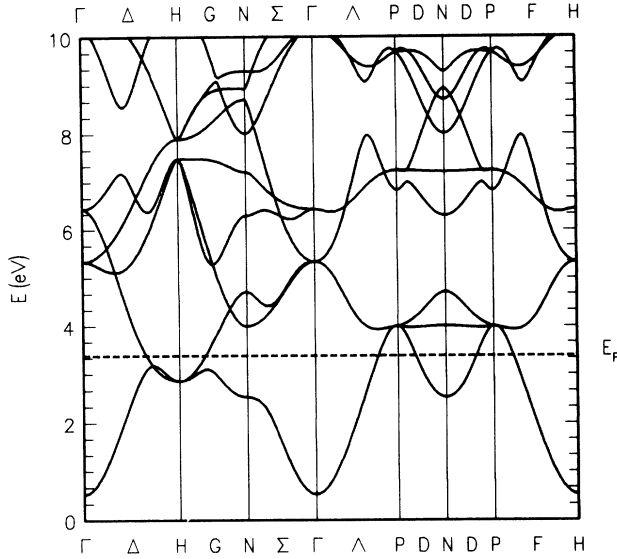


FIG. 1. The Slater-Koster band structure of bcc Ba. The Fermi energy is  $E_F = 3.377$  eV.

with both coarser and finer grids of  $\mathbf{k}$  points indicate that convergence has been reached with the grid used.

To extract the phonon spectrum from the dynamical matrix, a modification of the force-constant model of Rai and Hemkar<sup>10</sup> is employed for the short-range contribution,  $D^{(0,1)}$ . This quantity is added to  $D^{(2)}$  and the total is diagonalized. However, in order to determine the elastic constants for the force-constant model, it is necessary to consider only the "short-range" contributions to the elastic constants. The "long-range" contributions are obtained from small- $q$  calculations of  $D^{(2)}$  using the relations

$$D_{11}^{(2)}(q, 0, 0) = \Omega_p c_{11}^{(2)} q^2, \quad (10a)$$

$$D_{22}^{(2)}(q, 0, 0) = \Omega_p c_{44}^{(2)} q^2, \quad (10b)$$

$$D_{12}^{(2)}(q, q, q) = \Omega_p (c_{12}^{(2)} + c_{44}^{(2)}) q^2, \quad (10c)$$

which are valid for  $q \ll 2\pi/a$ , where  $\Omega_p$  is the primitive cell volume. The elastic constant contributions  $c^{(2)}$  are then subtracted from the corresponding experimental elastic constants<sup>16</sup> to obtain the "short-range" ones. The only other parameter used in the model is the experimental phonon frequency at the  $H$  point which is used to anchor the computed spectrum at that point.

## II. RESULTS AND DISCUSSION

The computed phonon spectrum of Ba is shown in comparison with the neutron-scattering data of Mizuki and co-workers<sup>1</sup> in Fig. 2. There is excellent agreement along the  $\Delta$  line as well as a predicted small feature in the longitudinal mode at  $0.6 \pi/a$  which is associated with Fermi surface nesting. Agreement is also very good along the other symmetry directions except for the longitudinal and upper transverse ( $T_2$ ) modes at the  $N$  point.

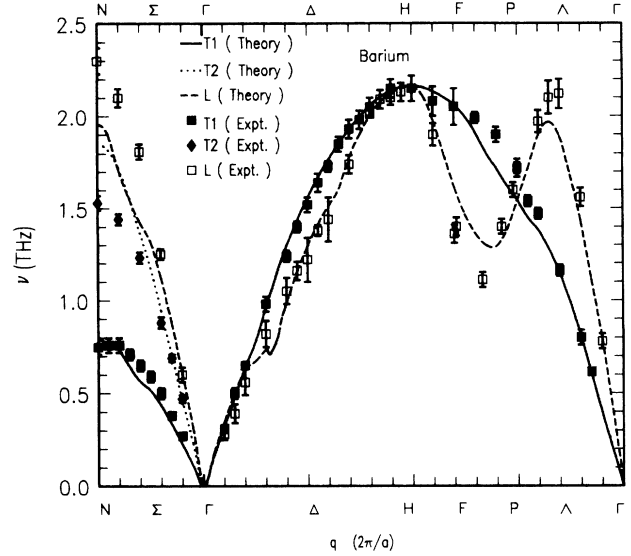


FIG. 2. The phonon spectrum of bcc Ba along the [100], [110], and [111] symmetry directions. The phonon frequency at the  $H$  point is 2.15 THz.

The relatively poor agreement here is due largely to having the computed spectrum and the experimental data match on the zone boundary only at the  $H$  point.

The computed spectrum behaves "normally" in the long-wavelength limit with the longitudinal mode lying above the transverse mode. The transition to anomalous behavior is found to occur along the  $\Delta$  line at about  $0.3\pi/a$ . It must be emphasized that features in the computed curve, apart from the long-wavelength limit and at the  $H$  point, do not specifically depend on experimental parameters. The anomalous features are due essentially to the long-range part of the dynamical matrix.

It is important to note that Fermi surface nesting is not responsible for the anomalous positioning of the longitudinal and transverse modes of the phonon spectrum in Ba along the  $\Delta$  line. This is because nesting of sheets of the Fermi surface will generally produce a small energy denominator in Eq. (2) over a significant region of the Brillouin zone and result in the sum exhibiting a cusp or peak. With the exception of the predicted minor anomaly at  $0.6\pi/a$  along the  $\Delta$  line, no such structure is seen in the spectrum. While nesting, often with states largely of  $d$  character, is typically responsible for observed anomalies in transition metals, the anomalous spectrum in Ba is due to  $d$ -state effects alone. Consequently, it is necessary to examine the matrix elements in Eq. (2). Since these appear as the product  $g^\alpha g^\beta$ , it is a straightforward but tedious matter to consider the mixings of the  $s$ ,  $p$ , and  $d$  contributions to  $D^{(2)}$ . This is achieved by calculating the individual terms of the electron-phonon coupling in Eq. (3) using only the  $s$ ,  $p$ , or  $d$  components of the eigenvectors before performing the Brillouin zone sum. This allows the separate contributions from the  $s$ - $s$ ,  $s$ - $p$ ,  $s$ - $d$ ,  $p$ - $p$ ,  $p$ - $d$ , and  $d$ - $d$  mixing terms to be identified in the computed  $D^{(2)}$ . In this way it is found that 87% of  $D^{(2)}$  at the  $H$  point is due to  $d$  interaction terms generally with 74% arising from  $p$ - $d$  and  $d$ - $d$  mixing terms and 13%

from  $s$ - $d$  mixing. At  $\pi/a$  along the  $\Delta$  line, the latter two percentages change to 84% and 7%, respectively, for the longitudinal mode and 75% and 11%, respectively, for the transverse mode.

As a second point, the longitudinal and transverse modes of  $D^{(2)}$  may be easily distinguished because the dynamical matrix is diagonal along the  $\Delta$  line. The longitudinal mode is in general significantly greater than the transverse mode along this line (except in the immediate vicinity of the  $H$  point and for small  $q$ ). Since  $D^{(2)}$  is negative with respect to  $D^{(0,1)}$ , this leads to the longitudinal mode lying lower in frequency than the transverse mode when the phonon spectrum is computed. Consequently, since  $d$  interaction terms form the majority contribution to  $D^{(2)}$  as noted in the previous paragraph, it may be inferred that  $d$ -state effects are primarily responsible for the anomalous phonon behavior of bcc Ba. This further supports the suggestion that this metal has more in common with its transition metal neighbors with regard to the electron-phonon interaction than would ordinarily be expected.

### III. CONCLUSIONS

A perturbative tight-binding formulation of the phonon dynamical matrix in which the long-range contribution is computed from first principles has been used to quantitatively reproduce the anomalous phonon spectrum of bcc Ba. The anomaly is found to be primarily due to  $p$ - $d$  and  $d$ - $d$  mixing effects, with a smaller contribution arising from  $s$ - $d$  mixing. This is in general agreement with several earlier nonperturbative calculations.<sup>2,3</sup> It may be concluded that Ba behaves as a "hybrid" between the simple and transition metals.

### ACKNOWLEDGMENTS

The authors appreciate discussions with Dr. J. L. Fry and Dr. G. Fletcher of the University of Texas at Arlington. One of us (K.S.) is grateful for the hospitality of the Department of Physics and Astronomy at Bates College where a portion of this work was carried out.

- 
- <sup>1</sup>J. Mizuki, Y. Chen, K.-M. Ho, and C. Stassis, *Phys. Rev. B* **32**, 666 (1985).  
<sup>2</sup>Y. Chen, K.-M. Ho, B. N. Harmon, and C. Stassis, *Phys. Rev. B* **33**, 3684 (1986).  
<sup>3</sup>J. A. Moriarty, *Phys. Rev. B* **34**, 6738 (1986).  
<sup>4</sup>Y. R. Wang and A. W. Overhauser, *Phys. Rev. B* **35**, 501 (1987).  
<sup>5</sup>A. O. E. Animalu, *Phys. Rev.* **161**, 445 (1967).  
<sup>6</sup>J. A. Moriarty, *Phys. Rev. B* **6**, 4445 (1977); **8**, 1338 (1973).  
<sup>7</sup>K. S. Sharma, *Phys. Status Solidi B* **108**, K101 (1981).  
<sup>8</sup>C. M. Varma, E. I. Blount, P. Vashishta, and W. Weber, *Phys. Rev. B* **19**, 6130 (1979).  
<sup>9</sup>C. M. Varma and W. Weber, *Phys. Rev. B* **19**, 6142 (1979); W. Weber, Habilitation Thesis, Universität Karlsruhe, 1984.  
<sup>10</sup>R. C. Rai and M. P. Hemkar, *J. Phys. F* **8**, 45 (1978). The force-constant model described in this reference is modified for use in the present paper by neglecting Rai and Hemkar's

approximate long-range contribution to the dynamical matrix (obtained in the free electron model); this leaves only the short-range contribution.

- <sup>11</sup>This is shown in Ref. 8 in the RPA. The generalization indicated here results from explicit expansion of the Coulomb vertex.  
<sup>12</sup>P. C. Pattnaik, M. E. Schabes, and J. L. Fry (unpublished).  
<sup>13</sup>D. A. Papaconstantopoulos, *Handbook of the Band Structures of Elemental Solids* (Plenum, New York, 1986).  
<sup>14</sup>W. A. Harrison, *Electronic Structure and the Properties of Solids* (Freeman, San Francisco, 1980).  
<sup>15</sup>J. L. Fry and P. C. Pattnaik, in *Integral Methods in Science and Engineering*, edited by F. R. Payne *et al.* (Springer-Verlag, New York, 1986).  
<sup>16</sup>U. Buchenau, M. Heiroth, H. R. Schober, J. Evers, and G. Oehlinger, *Phys. Rev.* **30**, 3502 (1984).